HEPATOLOGY
Official Journal of the American Association for the Study of Liver Diseases

Lineage-Dependent Effects of Aryl Hydrocarbon Receptor Agonists Contribute to Liver Tumorigenesis

Joshua A. Harrill,[1] Bethany B Parks,[1] Eliane Wauthier,[2] J. Craig Rowlands,[3] Lola M. Reid,[2]* and Russell S. Thomas[1]*

Rodent cancer bioassays indicate that the aryl hydrocarbon receptor (AHR) agonist, 2,3,7,8-tetracholorodibenzo-*p*-dioxin (TCDD), causes increases in both hepatocytic and cholangiocytic tumors. Effects of AHR activation have been evaluated on rodent hepatic stem cells (rHpSCs) versus their descendants, hepatoblasts (rHBs), two lineage stages of multipotent, hepatic precursors with overlapping but also distinct phenotypic traits. This was made possible by defining the first successful culture conditions for *ex vivo* maintenance of rHpScs consisting of a substratum of hyaluronans and Kubota's medium (KM), a serum-free medium designed for endodermal stem/progenitor cells. Supplementation of KM with leukemia inhibitory factor elicited lineage restriction to rHBs. Cultures were treated with various AHR agonists including TCDD, 6-formylindolo-[3,2-b]carbazole (FICZ), and 3-3'-diindolylmethane (DIM) and then analyzed with a combination of immunocytochemistry, gene expression, and high-content image analysis. The AHR agonists increased proliferation of rHpSCs at concentrations producing a persistent AHR activation as indicated by induction of *Cyp1a1*. By contrast, treatment with TCDD resulted in a rapid loss of viability of rHBs, even though the culture conditions, in the absence of the agonists, were permissive for survival and expansion of rHBs. The effects were not observed with FICZ and at lower concentrations of DIM. *Conclusion:* Our findings are consistent with a lineage-dependent mode of action for AHR agonists in rodent liver tumorigenesis through selective expansion of rHpSCs in combination with a toxicity-induced loss of viability of rHBs. These lineage-dependent effects correlate with increased frequency of liver tumors. (HEPATOLOGY 2015;61:548-560)

The aryl hydrocarbon receptor (AHR) is a ligand-activated transcription factor from the basic-helix-loop-helix/Per-ARNT-Sim (bHLH/PAS) superfamily.[1] Ligand activation triggers nuclear translocation of the receptor, dissociation of AHR from a HSP90/AIP/p23 multi-protein chaperone complex, and dimerization with aryl hydrocarbon receptor nuclear translocator (ARNT). The activated AHR/ARNT complex binds dioxin-response elements (DREs) in the upstream promoter of AHR-regulated genes and modulates their expression.[1] AHR regulates a diverse array of target genes including xenobiotic metabolizing enzymes,[1] cell cycle proteins,[2] ribosyltransferases,[3] and others.[1] Ligands for AHR include persistent organic pollutants such as 2,3,7,8-tetracholorodibenzo-p-dioxin (TCDD) and other polyhalogenated and nonhalogenated polycyclic aromatic hydrocarbons, tryptophan UV-photoproducts (FICZ), dietary indole-3-carbanol derivatives (DIM), and molecules endogenous to the liver such as 3-indoxyl sulfate.[1,4,5]

Potent xenobiotic AHR ligands, such as TCDD (Supporting Fig. S1), produce toxicities in rodents, including hepatotoxicity, immune suppression, epithelial hyperplasia, and tumor promotion in multiple tissues.[1] Activation of AHR (Fig. S2) is a key event in these toxicities given that AHR knockout mice are

Abbreviations: AHR, aryl hydrocarbon receptor; ARNT, aryl hydrocarbon receptor nuclear translocator; bHLH/PAS, basic-helix-loop-helix/Per-ARNT-Sim; BTSCs, biliary tree stem cells; DIM, 3-3'-diindolylmethane; DREs, dioxin-response elements; FICZ, 6-formylindolo-[3,2-b]carbazole; HBs, hepatoblasts; HpSCs, hepatic stem cells; KM, Kubota's medium; PBGs, peribiliary glands; rHpSCs, rodent hepatic stem cells; cells; TCDD, 2,3,7,8-tetracholorodibenzo-p-dioxin..

From the [1]Institute for Chemical Safety Sciences, Hamner Institutes for Health Sciences, Research Triangle Park, NC; [2]Program in Molecular Biology and Biotechnology, Department of Cell Biology and Physiology, UNC School of Medicine, Chapel Hill, NC; [3]Dow Chemical Company, Midland, MI.

Received March 21, 2014; accepted September 18, 2014.

Additional Supporting Information may be found at onlinelibrary.wiley.com/doi/10.1002/hep.27547/suppinfo.

**Coequal senior authors.*

insensitive to TCDD-mediated effects.[6,7] Chronic administration of TCDD to female rats produces pathological changes including hepatocellular hypertrophy, an increased frequency of multinucleated hepatocytes, proliferation of hepatic stem/progenitors, and infiltration of them into the hepatic lobule.[8,9] The pathological changes culminate in both hepatocytic and cholangiocytic tumors,[8] implicating TCDD-induced oncogenic effects on hepatic stem/progenitors.[10,11]

Lineage stages of hepatic parenchyma and their partner mesenchymal cells begin with biliary tree stem cells (BTSCs) in peribiliary glands (PBGs)[12]; transitioning to hepatic stem cells (HpSCs) and hepatoblasts (HBs) in/near canals of Hering[13]; continuing to acinar plates of parenchymal cells; and ending with terminally differentiated cells pericentrally.[14] Phenotypic properties change stepwise, correlating with gradients in matrix chemistry and other paracrine signals. Stem cell niches are enriched in hyaluronans, fetal laminins, and collagens, and proteoglycans with negligible/low levels of sulfation.[15] Extensive characterizations *in vitro* and *in vivo* of hBTSCs, hHpSCs, hHBs, and rHBs are summarized in many articles/reviews.[16,17] (See online supplement for further references.) Here we show that marker analyses for HpSCs versus HBs in humans and rodents are almost identical (Supporting Table S3).

In vitro evidence for regulation of progenitor functions by AHR is limited to studies using a transformed liver progenitor-like cell line (i.e., WB-F344 cells) in which AHR activation correlates with proliferation through loss of contact-mediated growth inhibition.[18,19] Increases in Jun D expression, cyclin A/cyclin-dependent kinase 2 (CDK2) activity, dysregulation of β-catenin signaling, and changes in cell-cell adhesion proteins were observed.[19-21] AHR activation has been shown to modulate cell cycle progression in other transformed cell lines.[1,10] The *in vitro* effects are consistent with the role of TCDD as a tumor promoter and indicate that AHR plays a role in regulating cell proliferation. However, the effects of AHR on HpSCs of any species have not been studied. Here we provide the first investigations of effects of AHR activation on rHpSCs versus rHBs using a combination of immunocytochemistry and high-content image analysis.

Materials and Methods

Most methods for cultures were as described previously.[15]

Rat Hepatic Stem Cell Cultures. Neonatal Sprague-Dawley rat livers were enzymatically dispersed and then cultured on substrata coated with 30 μg/cm^2 hyaluronan and in Kubota's medium (KM).[22] Recombinant rat leukemia inhibitory factor (LIF) was added at concentrations specified in experiments resulting in lineage restriction to hepatoblasts.

Chemical Treatments. AHR agonists were prepared in dimethyl sulfoxide (DMSO) at a 1,000× concentration and administered at 1 μL/mL of medium.

Assays. Cultures were analyzed using immunocytochemistry (ICC),[15] quantitative reverse-transcription polymerase chain reaction (qRT-PCR),[23] and high content image analyses.[24] (See online supplement for details of the methods.)

Results

Hyaluronans: Essential Conditions for rHpSCs. Neonatal rat liver cells were plated into KM and onto collagen types III, IV, or plastic. Mesenchymal cells rapidly overgrew cultures, reaching confluence within a week; parenchymal cell growth was limited (Fig. S5). In contrast, plating onto hyaluronans and in KM resulted in coordinated growth responses of parenchymal and mesenchymal cells (Fig. 1A). By 10–12 days, cells had formed distinct stem/progenitor colonies (Fig. 1A). Colony sizes increased, indicating proliferation, and contained both epithelial and mesenchymal cells. Hepatic lineage markers previously established for either hHpSCs and hHBs or rHBs (Supporting Table S3) were used to characterize the cultures using immunocytochemistry. Both epithelial and mesenchymal cells were positive for CD44, the hyaluronan receptor (Fig. 1B). The epithelial, but not mesenchymal cells, were positive for E-cadherin, EpCAM, and

Address reprint requests to: Joshua A. Harrill, Ph.D., Center for Toxicology and Environmental Health, 5120 North Shore Dr., North Little Rock, AR 72118. E-mail: JHarrill@cteh.com or Lola M. Reid, Ph.D., Glaxo Building, Rm. 34; 101 Mason Farm Rd., UNC School of Medicine, Chapel Hill, NC 27599. E-mail: Lola.M.Reid@gmail.com

View this article online at wileyonlinelibrary.com.

DOI 10.1002/hep.27547

Potential conflict of interest: Dr. Reid consults, received grants, and holds intellectual property rights with Vesta Therapeutics. She consults, owns stock, and holds intellectual property rights with PhoenixSongs Biologicals. She received grants from Dow Chemical. Dr. Thomas received grants from Dow Chemical.

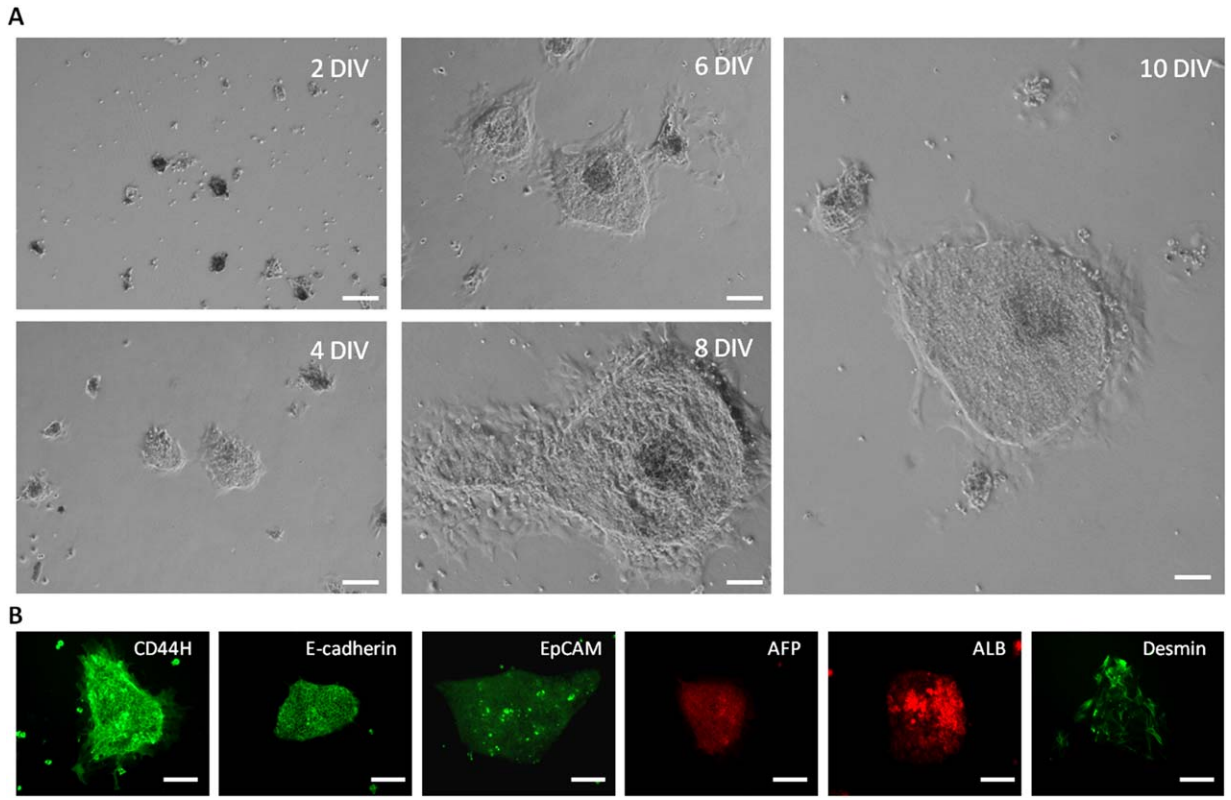

Fig. 1. Hyaluronan promoted selective expansion of rat hepatic stem/progenitor cells *in vitro*. Cell suspensions from PND0-2 rat livers were seeded in KM and on 30 $\mu g/cm^2$ hyaluronan. At 2 days *in vitro*, unbound cells were rinsed away and selective attachment of small clusters of cells was observed. (A) Serial imaging of an attached cell cluster between 2 and 10 days *in vitro*. By 10 days *in vitro*, attached cell clusters formed discrete two-dimensional colonies of hepatic stem/progenitor cells in close association with a population of mesenchymal precursors, operating as feeders. (B) Rat hepatic stem/progenitor colonies cultured for 6 days *in vitro* were examined for expression of CD44H, E-cadherin, EpCAM, AFP, ALB, and desmin using immunocytochemistry. Scale bars = 100 μm.

scattered cells for alpha-fetoprotein (AFP) and/or albumin (ALB) (Fig. 1B). These phenotypic traits are consistent with mixed cultures of rHpSCs and of rHBs. Mesenchymal cells coexpressing desmin and CD44 were hepatic stellate precursors (Fig. 1B) as defined previously.[15] Adult rat hepatocytes did not express EpCAM, AFP, or CD44 (Fig. S6). ALB and E-cadherin were expressed by hepatocytes but with a distinct expression pattern as compared to stem/progenitors. Occasional desmin+ mesenchymal cells were observed. Thus, hyaluronans plus KM supported survival and expansion of hepatic stem/progenitors and their mesenchymal partners. Expansion varied from stable, steady cell divisions for most colonies to some with limited divisions followed by degeneration due, we assume, to stem cells present in stable colonies versus committed progenitors in those that degenerated.

LIF Enhances Lineage Restriction to and Expansion of rHBs. LIF is an interleukin-6 (IL-6) family cytokine used to promote expansion of murine embryonic stem (ES) cells and is a potent paracrine signal produced by angioblasts and stellate precursors.[15,25] LIF increased desmin+ cell proliferation and, in parallel, lineage restriction to rHBs (Fig. 2A). The time course of mesenchyal precursor and hepatic stem/progenitor cell growth was quantified in response to varying concentrations of LIF (0-10 ng/mL) using high-content imaging. Concentration-dependent increases in total numbers (Fig. 2B) and areas (Fig. 2C) of desmin+ cells per well were observed at 6, 9, and 12 days *in vitro*. For each measurement, the threshold for statistically significant increases in mesenchymal precursors was 1 ng/mL with a plateau in effects observed between 5-10 ng/mL. Similarly, a concentration-dependent increase in hepatic stem/progenitor-colony areas (Fig. 2D), number of cells/colony (Fig. 2E), and average number of colonies/well (Fig. 2F) were also observed. Marked increases in colony area and number of cells/colony occurred at 12 days *in vitro* at LIF concentrations $\geq$0.5 ng/mL. A less pronounced effect was observed at 9 days *in vitro* at LIF concentrations of $>$1 ng/mL (Fig. 2D,E). A significant increase in the number of hepatic stem/progenitor colonies/well was observed with 0.5-10 ng/mL LIF at

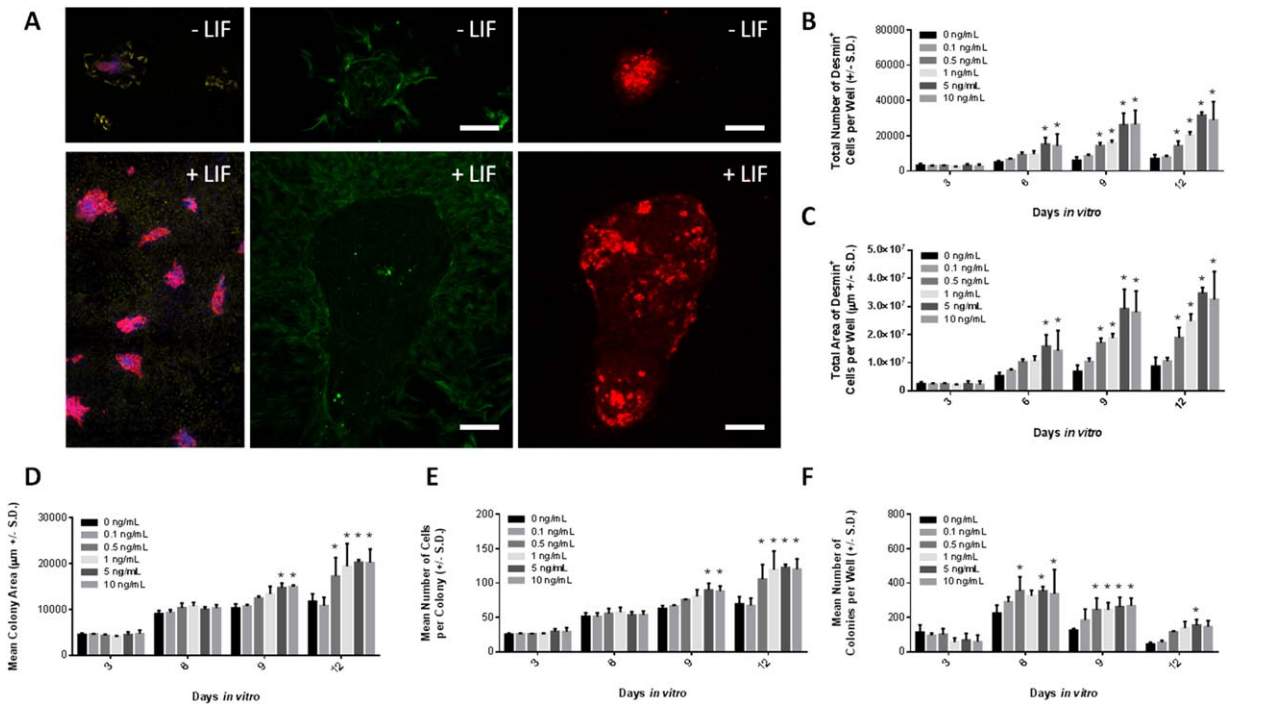

Fig. 2. LIF enhanced the growth of rat hepatic stem/progenitors and mesenchymal precursor cells. (A) Rat hepatic stem/progenitors were cultured on 30 $\mu g/cm^2$ hyaluronan for 12 days *in vitro* in KM (top row) or KM + 10 ng/mL LIF (bottom row). Cultures were immunolabeled with antibodies against desmin (green), ALB (red) and E-cadherin (not shown). Left panels are low-magnification images demonstrating the marked increase in hepatic stem/progenitor and mesenchymal precursor growth in the presence of LIF. Higher-magnification images of desmin and ALB labeling in colonies grown in the absence or presence of LIF are to the right. Scale bars = 100 μm. (B) Total number of desmin+ cells per well as determined by nuclear quantification. (C) Total area of desmin-positive cells per well. (D) Mean hepatic stem/progenitor colony area (μm^2), derived from E-cadherin labeling. (E) Mean number of cells per colony. (F) Mean number of hepatic stem/progenitor cell colonies per well. For all graphs, the bars represent the mean of three wells/group collected across three independent cultures. The error bars represent the standard deviation across the three independent cultures. *Significantly different from 0 ng/mL LIF condition within each timepoint ($P < 0.05$, Tukey's multiple comparison test).

6 and 9 days *in vitro* (Fig. 2F). This effect was less pronounced at 12 days. The data indicated that LIF enhanced growth of mesenchymal precursors and facilitated survival of rHBs. For subsequent experiments, a concentration of 1 ng/mL LIF was used.

LIF-Supplemented Cultures Consisted Primarily of rHBs. Fluorescent co-labeling with E-cadherin and ALB demonstrated that LIF-supplemented cultures were primarily rHBs (Fig. 3; Fig. S3). The rHpSC colonies, those dominating in LIF-negative cultures, were composed exclusively of tightly-packed cells with little cytoplasm, cell surface expression of E-cadherin at intercellular contact sites, and scattered cells with low or no ALB expression (Fig. 3A, top row), phenotypic traits consistent with those of HpSCs.[20] The rHB colonies were comprised of cells with larger cytoplasmic area, diffuse E-cadherin expression, and with all cells expressing ALB and at higher levels (Fig. 3A, middle row) and AFP (data not shown), phenotypic traits typical of HBs.[13,22] The third type of colony contained a mixture of rHpSCs and rHBs. The colony (Fig. 3A, bottom row) shows rHpSCs giving rise to a cord of rHBs.

Variations in patterns of E-cadherin and ALB immunolabeling were leveraged to quantitatively distinguish rHpSC and rHB colony types using high-content imaging. Scatterplots of E-cadherin and ALB fluorescent surface area densities (FSAD) for colonies grown in the presence or absence of 1 ng/mL LIF (Fig. 3B) comprise data in which each point represents an individual colony. Beginning at 9 days *in vitro*, a distinct difference was noted in LIF+ versus LIF– cultures. In LIF+ cultures, colonies with high ALB differential intensity values were observed, and these were largely absent in LIF– cultures (Fig. 3B, red oval). The differences were more pronounced at 12 days *in vitro*. Both culture conditions contained colonies with high E-cadherin differential intensity values (Fig. 3B, green oval).

Bipartite gating of E-cadherin and albumin FSAD values demonstrated that rHpSCs and rHB colonies could be separated and quantified independently (Fig. 4A,B). Colonies with high ALB and low E-cadherin FSADs had morphologies consistent with rHBs (Fig. 4C, left column). Colonies with the inverse relationship

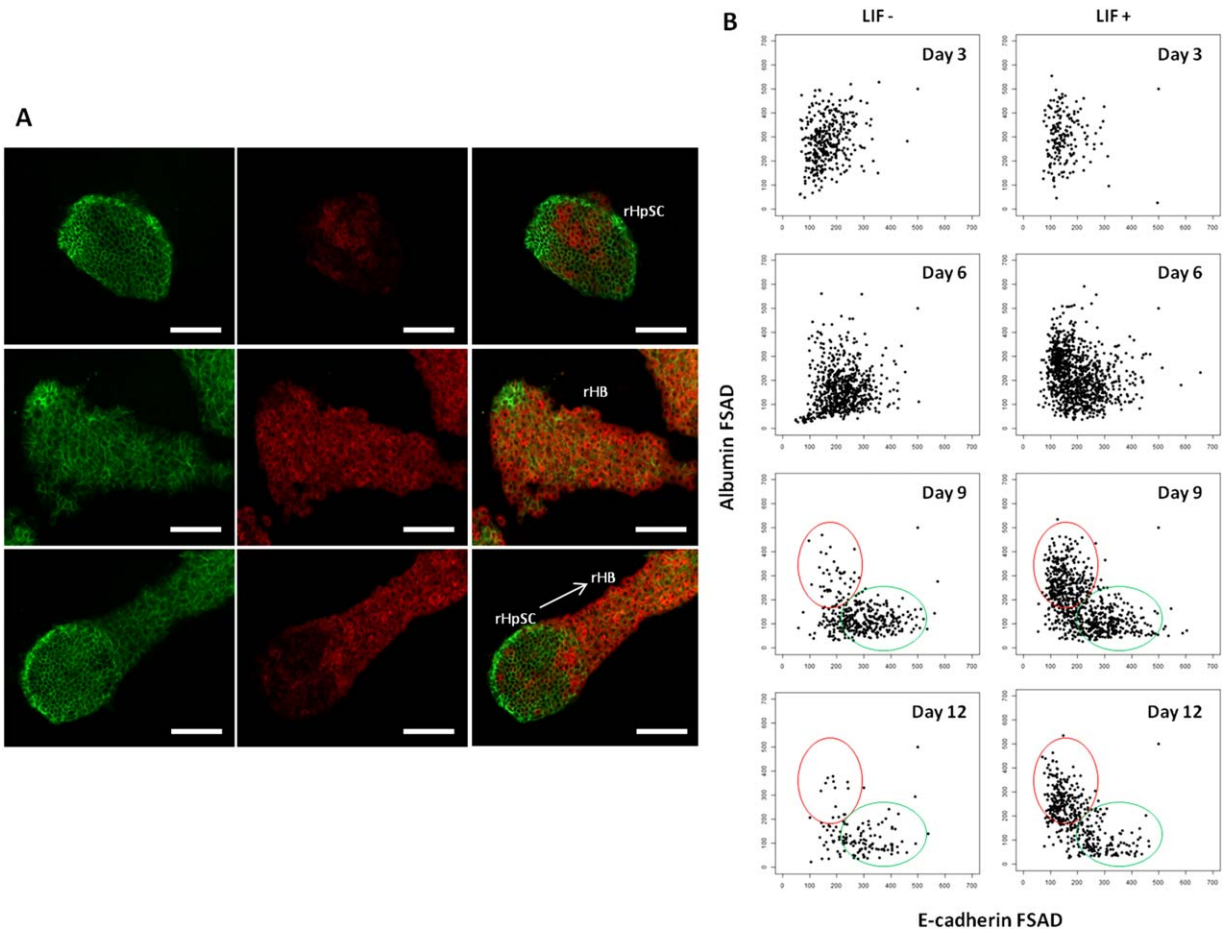

Fig. 3. LIF promoted the growth of colonies enriched with rHBs. Rat hepatic stem/progenitors were cultured on 30 μg/cm^2 hyaluronan in KM supplemented with 1 ng/mL LIF. (A) At 12 days *in vitro*, cultures were immunolabeled with E-cadherin (green) and albumin (red). Columns of images from left to right are as follows: E-cadherin label (green), albumin label (red), and merged fluorescent images. Each row corresponds to matching images from the same colony. Top row: Consistent with the phenotypic traits of rHpSCs. Middle row: Consistent with traits of rHBs. Bottom row: Consistent with a mixed phenotype colony containing both rHpSCs and rHBs; the rHpSC component of the colony is giving rise to a cord of rHBs oriented toward the upper right of the image. Scale bars = 100 μm. (B) Analysis of E-cadherin and ALB fluorescent surface area densities (FSAD) demonstrates emergence of discrete colony types in the presence of LIF. At 3, 6, 9, and 12 days *in vitro*, LIF– and LIF+ cultures were immunolabeled with E-cadherin and ALB. Cultures were imaged and analyzed using high-content image analysis. Panels are scatterplots of E-cadherin (x-axis) and ALB (y-axis) FSADs with time in LIF– (left) and LIF+ (right) cultures. Each point represents an individual colony. In the presence of LIF, two discrete populations of colonies emerge at 9 days *in vitro* and persist at 12 days *in vitro*. This phenomenon is not observed in the absence of LIF (compare red ovals across columns). Colony data were pooled across three replicate wells from three independent cultures.

(low ALB and high E-cadherin FSADs) had morphologies consistent with rHpSCs (Fig. 4C, right column). Neither the number of rHpSC colonies (Fig. 4A,B, green bubbles) nor the population distribution of rHpSC colony area measurements (Fig. 4D,E, green boxplots) was affected by the presence or absence of LIF. In contrast, rHB colonies were essentially absent in LIF– cultures (Fig. 4A, red bubbles), whereas large numbers were present in LIF+ conditions (Fig. 4B, red bubbles). Quantitatively, the upper limit of the population distribution of rHB colony area measurements was greatly increased in LIF+ as compared to LIF– cultures (Fig. 4D,E, red boxplots), indicating a stimulatory effect of LIF on rHB growth.

Quantitative RT-PCR profiling with stage-specific markers supported the morphological and immunocytochemical results demonstrating the stimulatory effects of LIF on rHB growth (Fig. 5). A summary of known hepatic lineage markers (online supplement, Supporting Table S3) indicates expression of markers in both HpSCs and HBs (e.g., *Epcam, Sox9*) (Fig. 5A,B) or in HpSCs but not HBs (e.g., *Ncam*) (Fig. 5C) or vice versa (e.g., *Afp*). *Ncam* increased between 3 and 12 days *in vitro* in LIF+ and LIF– cultures. Expression of HBs' markers (e.g., *Afp*, *Alb*) were minimal in LIF– cultures but increased or remained constant in LIF+ cultures over time (Fig. 5D,E), concurrent with the expansion of rHBs stimulated by LIF (Fig. 4). Expression of BTSC

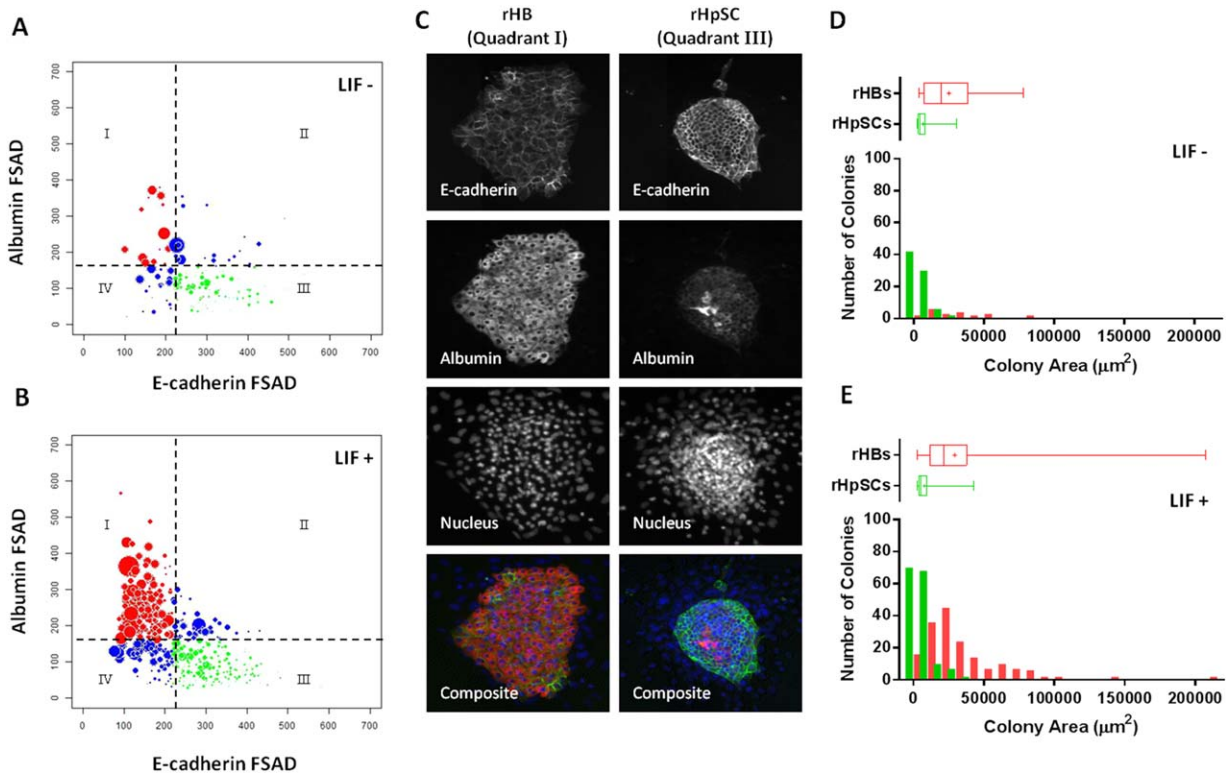

Fig. 4. High-content image gating analysis and quantification of rHpSC and rHB colony populations. (A,B) Bubble plots of E-cadherin (x-axis) and ALB (y-axis) FSADs at 12 days *in vitro* in the absence (LIF–) or presence (LIF+) of 1 ng/mL LIF. Each bubble represents an individual colony. The size of the bubble is proportional to the size of the colony. A bipartite gate was installed which separates a majority (>85%) of colonies into populations with morphology consistent with either rHBs or rHpSCs. Red bubbles = rHBs. Green bubbles = rHpSCs. Blue bubbles = not classified. Note the near absence of rHB colonies in cultures maintained in the absence of LIF. (C) Representative images of rHB (left column) and rHpSC (right column) colony morphology at 12 days *in vitro* in the presence of 1 ng/mL LIF. Note the differences in E-cadherin and albumin labeling patterns between colony types. (D,E) Box-and-whisker plots and corresponding histograms for rHB (red) and rHpSC (green) colony subpopulations in the absence (LIF–) or presence (LIF+) of 1 ng/mL LIF. Stems are the minimum and maximum of colony area measurements. Vertical line = population median. + = population mean. Boxes represent the first and third quartiles. Colony data were pooled across three replicate wells from three independent cultures.

markers (e.g., *Sox17*) decreased over time in both LIF+ and LIF– cultures (Fig. 5F). Together, the data from high-content imaging and qRT-PCR indicate that LIF is a requirement for rHBs but not for rHpSCs.

AHR Expression and AHR-Mediated Gene Induction in Rat Hepatic Stem/Progenitors. The expression of *Ahr* and two genes, *Ahrr* and *Cyp1a1*, whose transcription is induced by AHR activation, were measured in LIF+ cultures versus hepatocytes (Fig. 6A-C). The *Ahr* transcript was detectable, albeit at lower levels than in hepatocytes. Expression levels remained constant between 3 and 12 days *in vitro* (Fig. 6A). *Ahrr* transcripts were detectable with ∼10-fold increase in expression observed between 3-12 days *in vitro* (Fig. 6B). *Ahrr* was not detected in hepatocytes. The *Cyp1a1* transcript was also detectable and increased beginning at 9 days *in vitro* (Fig. 6C). At 3 and 6 days *in vitro*, *Cyp1a1* expression levels were comparable to that observed in hepatocytes. By 9 and 12 days *in vitro, Cyp1a1* expression was 50-100 times greater than hepatocytes.

Transcriptional activation of AHR in stem/progenitors was assessed by measuring induction of *Cyp1a1* mRNA following acute exposure to three different AHR agonists—TCDD, FICZ, and DIM (Fig. 6D-F). Cultures were grown with 1 ng/mL LIF for 12 days *in vitro* and then exposed to multiple concentrations of the test chemicals for 4, 24, 48, and 96 hours. In the sham (U) or vehicle (V) treatment groups, *Cyp1a1* mRNA decreased over time. Concentrations of TCDD between 0.1 and 100 nM increased *Cyp1a1* mRNA 400 to 600-fold by 24 hours; it remained elevated for the duration of the experiment (Fig. 6D). FICZ at concentrations of 10 and 100 nM produced a similar persistent induction of *Cyp1a1* mRNA as observed with TCDD. At lower concentrations of 0.1 and 1 nM FICZ, a transient induction of *Cyp1a1* mRNA occurred (Fig. 6E). DIM at concentrations of 1 and

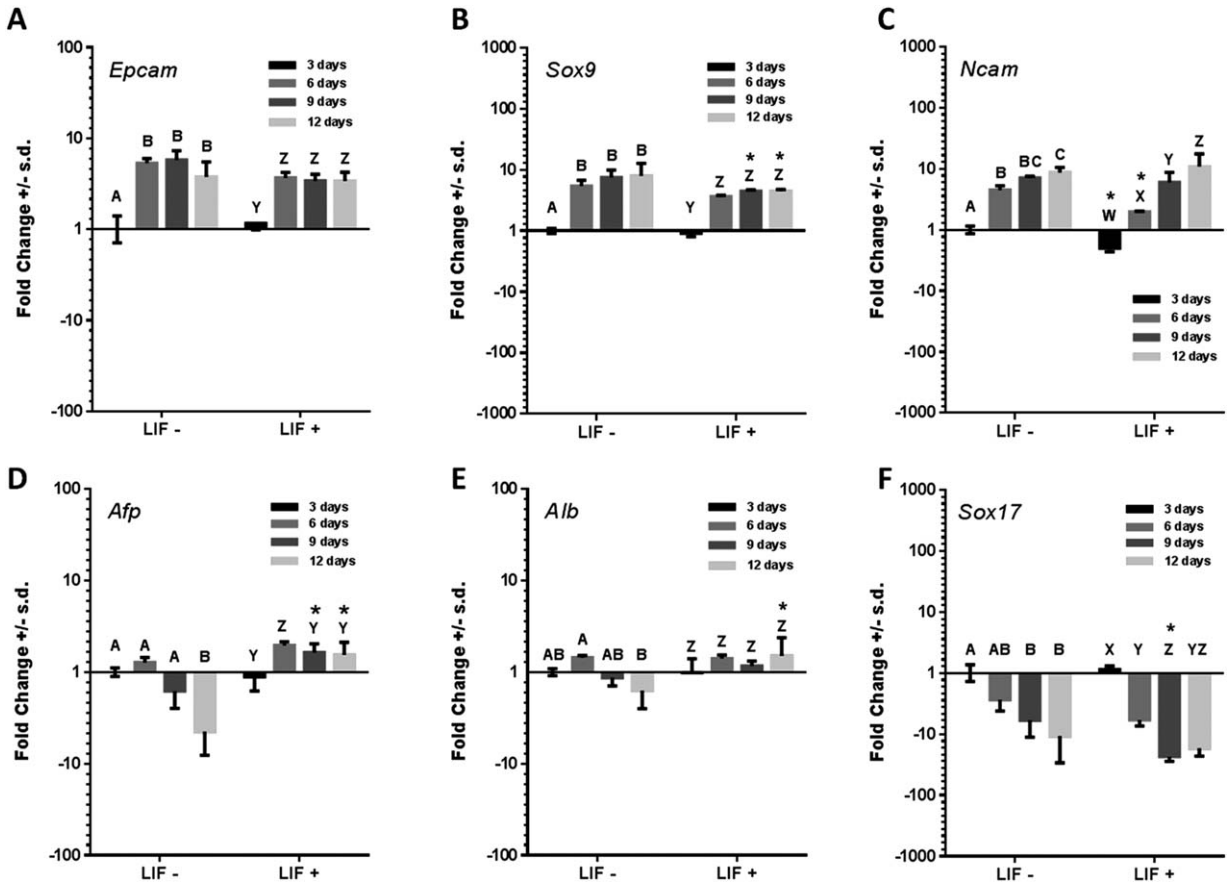

Fig. 5. Time course expression of rHpSC and rHB markers with and without LIF supplementation. Rat hepatic stem/progenitors were cultured on 30 $\mu g/cm^2$ hyaluronan in KM in the presence (LIF+) or absence (LIF–) of 1 ng/mL LIF. At 3, 6, 9, and 12 days *in vitro*, RNA was extracted and analyzed using TaqMan qRT-PCR. Data are expressed as fold-changes from LIF– cultures at 3 days *in vitro*. For all graphs, the bars represent the mean of three wells/group collected across three independent cultures. The error bars represent the standard deviation across the three independent cultures. (A) *Epcam*, (B) *Sox9*, (C) *Ncam*, (D) *Afp*, (E) *Alb*, (F) *Sox17*. Data for each gene were analyzed using a two-way analysis of variance (ANOVA) followed by Sidak's multiple comparison test for treatment effects within each timepoint and Tukey's multiple comparison test for effects of time within each treatment group. For each gene, within each treatment, bars labeled with the same letter were not significantly different from one another (Tukey, $P < 0.05$). Bars denoted with stars indicate a significant difference from the matching timepoint in the absence of LIF.

10 μM produced persistent induction of *Cyp1a1* mRNA, albeit at lower levels than that observed with FICZ or TCDD. DIM at 0.1 μM did not increase *Cyp1a1* mRNA expression. DIM was cytotoxic to both rHpSCs and rHBs at 100 μM (data not shown). Thus, AHR is expressed in rat hepatic stem/progenitors and can be activated in response to various ligands.

AHR Agonists Affect the Growth Characteristics of Rat Hepatic Stem/Progenitor Cultures. Rat hepatic stem/progenitors were treated with three different AHR agonists (TCDD, FICZ, and DIM) from 2-12 days *in vitro* and analyzed for changes in growth, morphology, and gene expression. Representative images from treated cultures (Fig. 7A) demonstrated that exposure to each AHR agonist produced a marked increase in growth of rHpSC colonies. Bubble plots (Fig. 7B) illustrate this phenotypic shift. Compared to sham or vehicle treatment, cultures exposed to AHR agonists had greater rHpSC colony sizes using E-cadherin and ALB FSAD measurements.

Growth characteristics of rHpSC and rHB colonies in response to varying concentrations of AHR agonists were quantified and summarized (Fig. 7C,D). TCDD at concentrations of 0.1 and 1 nM produced a significant difference in the distribution of rHpSC colony area measurements as compared to vehicle controls (Fig. 7C). The mean colony area increased, as did the third quartile of colony area measurements, indicating a net increase in rHpSCs. Similar effects were observed with FICZ and DIM at concentrations ranging from 1 to 100 nM and 1 to 10 μM, respectively. TCDD at concentrations of 10 and 100 nM did not affect the rHpSC colony area measurements, but this may be

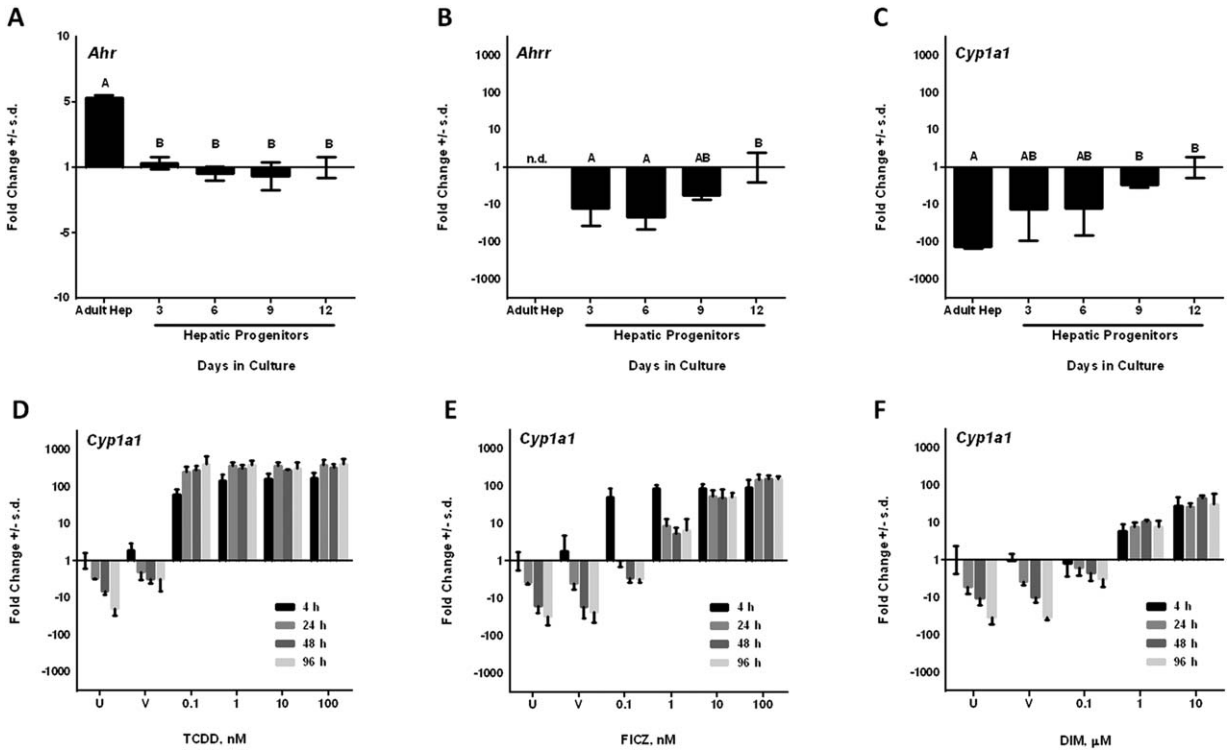

Fig. 6. Expression of Ahr, AHR-responsive genes, and treatment-related increases in Cyp1a1 mRNA in rat hepatic stem/progenitors. (A-C) Rat hepatic stem/progenitors were cultured on 30 μg/cm^2 hyaluronan in KM in the presence of 1 ng/mL LIF. At 3, 6, 9, and 12 days *in vitro*, expression of Ahr (A), Ahrr (B), and Cyp1a1 (C) was measured using TaqMan qRT-PCR. Expression of Ahr, Ahrr, and Cyp1a1 was also measured in hepatocytes isolated from an adult rat liver. Data are expressed as fold-change from cultures sampled at 12 days *in vitro*. For all graphs, the bars represent the mean of data from three wells/group collected across three independent cultures. The error bars represent the standard deviation across the three independent cultures. Data for each gene were analyzed using a one-way ANOVA followed by a Tukey's multiple comparison test. Bars labeled with the same letter were not significantly different from one another (Tukey, $P < 0.05$). (D-F) Rat hepatic stem/progenitors were cultured on 30 μg/cm^2 hyaluronan in the presence of 1 ng/mL LIF for 12 days. At 12 days *in vitro*, cultures were treated with varying concentrations of AHR agonists and expression of Cyp1a1 was measured using TaqMan qRT-PCR at 4, 24, 48, and 96 hours after exposure. Data are expressed as fold-change from sham-treated cultures at 4 hours. For all graphs, bars represent the mean of three wells/group collected across three independent cultures. Error bars represent the standard deviation across the three independent cultures.

due to the overall decrease in colony numbers per well (data not shown).

A significant difference in rHB colony area measurements was observed with TCDD treatment. The mean and third quartile of rHB colony area measurements were decreased as compared to vehicle controls (Fig. 7D). A similar effect on the distribution of rHB colony area was observed with DIM at concentrations of 1 and 10 μM, but not with FICZ. Thus, there was a net decrease in rHB colony growth with TCDD and the two highest concentrations of DIM.

Expression levels of *Epcam* mRNA (marker of both HpSCs and HBs[20,31]) in cultures treated with AHR agonists were consistent with lineage-stage-specific effects observed using high content imaging (Fig. 7E). Treatment with TCDD showed a nonmonotonic increase in *Epcam* mRNA with a maximal increase at 0.1 nM followed by a decrease at higher concentrations. *Epcam* expression was still greater than controls at the higher TCDD concentrations. Treatment with FICZ and DIM showed monotonic increases in *Epcam* mRNA. The concentration-dependent responses in *Epcam* expression for each agonist were consistent with increased selection and growth of rHpSCs and, in the case of TCDD, decrease in rHB growth at the higher concentrations tested.

A similar relationship between high content imaging and gene expression data for TCDD was observed for *Afp*, *Alb*, and *Sox17* (Fig. 7E). TCDD treatment decreased expression of both *Afp* and *Alb*, indicating a marked loss of rHB colonies. FICZ treatment caused increased expression in *Epcam*, a decrease in *Alb*, and, at the highest concentration, an increase in *Sox17*, effects paralleling those of TCDD; paradoxically, it also resulted in a modest increase in *Afp* expression (Fig. 7E). Treatment with DIM showed similar changes, but the effects were more muted and not statistically significant (Table 1).

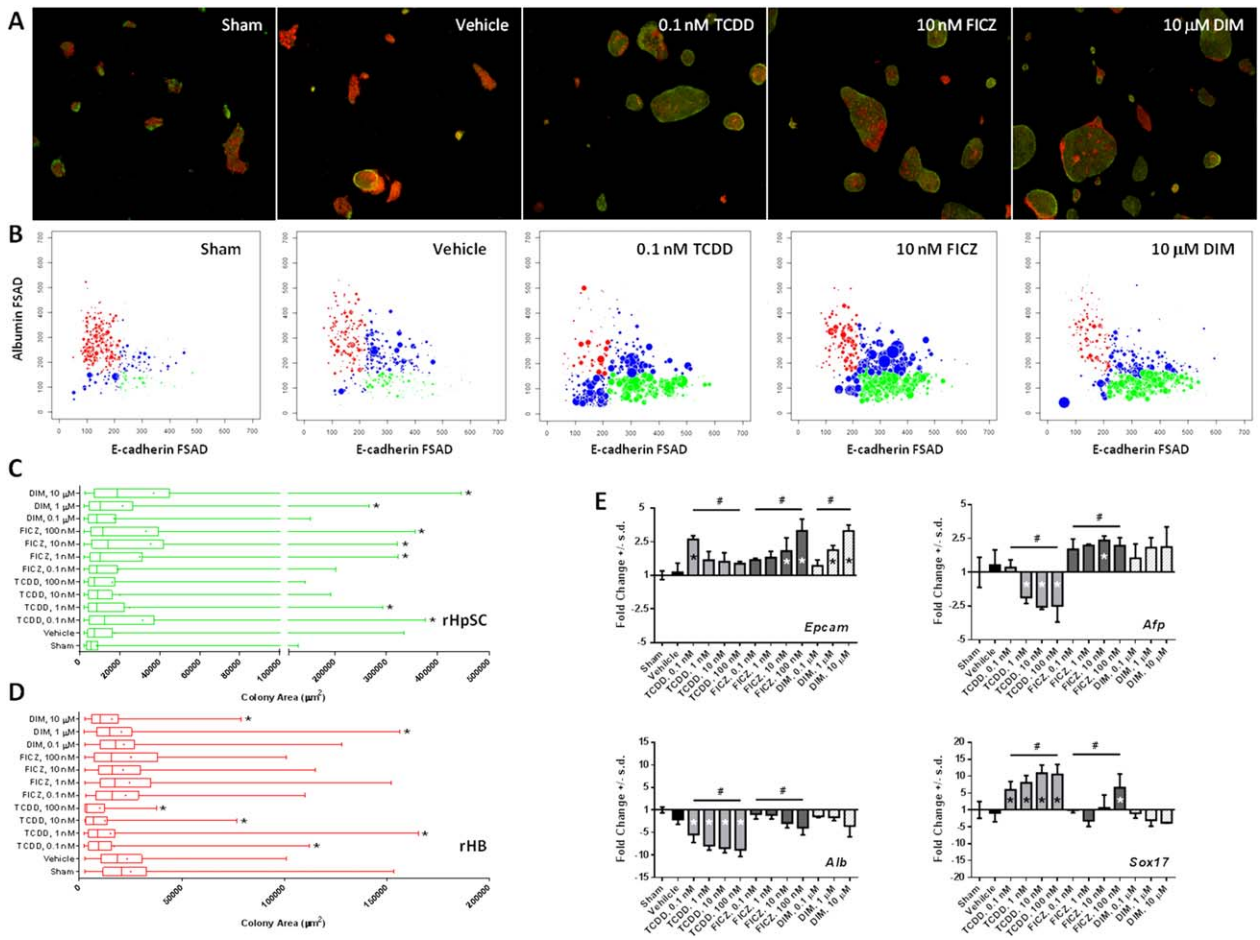

Fig. 7. AHR agonists affect the growth of rat hepatic stem/progenitors. Rat hepatic stem/progenitors were cultured on 30 μg/cm^2 hyaluronan in KM plus 1 ng/mL LIF. At 2, 5, 8, and 11 days *in vitro*, media changes were performed with media containing various concentrations of AHR agonists (TCDD, FICZ, DIM). Cultures were sampled at 12 days *in vitro* for either high-content imaging or qRT-PCR analysis. (A). Representative images of hepatic stem/progenitor cultures from high-content image analysis. Red = ALB, green = E-cadherin. (B) Bubble plots of E-cadherin (x-axis) and ALB (y-axis) FSADs. Each bubble represents an individual colony. The size of the bubble is proportional to the size of the colony. Gates are those described in Fig. 5. Red bubbles = rHBs, green bubbles = rHpSCs, blue bubbles = unclassified. (C,D) Box-and-whisker plots of colony area for colonies classified as rHpSCs (C) or rHBs (D). Stems are the minimum and maximum of colony area measurements. Boundaries of the box are the first and third quartiles. Vertical line = median colony area measurement. + = mean colony area measurement. *Distribution of colony areas is significantly different from vehicle ($P < 0.05$, Mann-Whitney rank sum test). (E) TaqMan qRT-PCR analysis of *Epcam*, *Sox17*, *Afp*, and *Alb* expression. Data are expressed as fold-change from untreated controls. For all graphs, the bars represent the mean of three wells/group collected across three independent cultures. The error bars represent the standard deviation across the three independent cultures. Data for each test chemical were analyzed by one-way ANOVA followed by Dunnett's mean contrast test comparing treated samples to vehicle. #$P < 0.05$, ANOVA. *$P < 0.05$, Dunnett's. Further details are in Table 1.

Discussion

To our knowledge, this is the first study in which successful culture conditions for rHpSCs have been identified. By contrast, rHBs survive *ex vivo* using classical culture conditions, including those with serum supplementation. The requirements for rHpSCs comprise a substratum of hyaluronans in combination with serum-free KM, a medium designed for endodermal stem/progenitors and one devoid of cytokines or growth factors.[16,22]

Hylauronans are polymers of D-glucuronic acid and D-N-actetylglucosamine disaccharides, dominant matrix components of stem cell niches and to which the stem/progenitors bind by way of CD44, a hyaluronan receptor. Mature cells do not express CD44. The rHpSCs and rHBs can be distinguished readily by numerous phenotypic traits and by distinct requirements for their survival and expansion *ex vivo*, findings similar to those for human hepatic stem/progenitors.[13,16] Examples include expression of NCAM only in rHpSCs; of AFP only in rHBs; minimal (if any) expression of ALB in rHpSCs versus in all and at much higher levels in rHBs. Similarly, E-cadherin, found in most hepatic parenchyma, demonstrated distinctions in cell packing

Table 1. Summary of High-Content Imaging and Gene Expression Data in Response to AHR Ligands

Treatment	Dosage	*Cyp1a1* Induction (Fold-Change)	rHpSCs		rHBs		qRT-PCR*			
			N†	Mean Area (μm²)	N†	Mean Area (μm²)	*Epcam*	*Sox 17*	*AFP*	*ALB*
Sham	–	None	123	8,526	207	25,011	n/a	n/a	n/a	n/a
Vehicle	–	None	229	17,692	172	23,301	–	–	–	–
TCDD	0.1 nM	Persistent (500)	243	31,551‡	77	16,858‡	Up	Up	–	Down
	1 nM	Persistent (500)	214	24,975‡	62	15,222‡	–	Up	Down	Down
	10 nM	Persistent (500)	143	20,136	39	12,498‡	–	Up	Down	Down
	100 nM	Persistent (500)	93	16,395	11	9,970‡	–	Up	Down	Down
FICZ	0.1 nM	Transient	150	19,411	121	22,610	–	–	–	–
	1 nM	Transient	251	30,117‡	186	24,477	–	–	–	–
	10 nM	Persistent (70)	332	35,574‡	125	21,337	Up	–	Up	–
	100 nM	Persistent (120)	194	33,194‡	56	25,221	Up	Up	–	–
DIM	0.1 μM	None	220	17,287	195	21,729	–	–	–	–
	1 μM	Persistent (9)	294	21,515‡	199	20,491‡	Up	–	–	–
	10 μM	Persistent (50)	356	37,007‡	160	15,860‡	Up	–	–	–

rHpScs = rat hepatic stem cells; rHBs = rat hepatoblasts.

*Gene expression data presented as directional change from vehicle control. – = no change. n/a = not applicable.

†N = number of colonies.

‡High content image analysis data. Significantly different from vehicle control ($P < 0.05$, Mann-Whitney rank sum test).

densities and distinct immunocytochemical labeling patterns: dense, cell surface localization of E-cadherin in rHpSCs and diffuse cell surface, and cytoplasmic localization of E-cadherin in rHBs. Intracellular E-cadherin and ALB staining patterns provided a means by which to separate and rapidly quantify the two lineage stages using a combination of automated image acquisition, high-content imaging, and a gating strategy similar to that used in single-cell flow cytometric analyses. Similar approaches have been used to analyze the heterogeneity of colony types in human and murine ES cell cultures exposed to various conditions.[24]

Hyaluronan receptors are a generic trait of stem/progenitors[26] and are found in a variety of isoforms resulting from alternative gene splicing.[27] Certain variants form multiprotein complexes with EpCAM, claudins, tetraspanins, and integrins and are associated with metastasis of liver, and other types of cancer.[28-31] CD44 expression in liver cancers is negatively associated with survival prognosis[31,32] and has been used to isolate human cholangiocarcinoma cancer stem cells.[33] In rat livers, CD44+ cells infiltrate hepatic acini in response to chemically induced liver injuries triggering hepatic stem/progenitor proliferation and EpCAM+ cells that can reconstitute damaged livers.[34] The rHpSCs and rHBS have coexpression of CD44 and EpCAM.

Supplementation with LIF resulted in expansion of desmin+ mesenchymal precursors and, in parallel, lineage restriction of rHpSCs to rHBs, due presumably to stellate precursor paracrine signaling. By contrast, paracrine signals from mature stellate cells result in lineage restriction to diploid, adult hepatocytes, so-called "small hepatocytes," corroborating prior reports.[15] Thus, expansion and survival conditions are lineage stage-specific in terms of matrix and soluble signals, a finding similar to that reported previously for human parenchymal cells.[15]

LIF stimulated proliferation of desmin+ mesenchymal precursors and, in parallel, lineage restriction of rHpSCs to rHBs. LIF, a member of the IL-6 growth factor family, is commonly used to promote expansion and suppress differentiation of murine ES cells.[35] The role(s) of LIF in rat liver development is not well defined. However, previous studies have demonstrated that LIF has a marked proliferative effect on precursors of endothelia and of vitamin-A-storing stellate cells.[25] Both fetal and adult rat hepatocytes express the LIF receptor, as shown by radioligand binding experiments with ^{125}I-LIF.[36] During chemically induced hepatic stem/progenitor responses, the expression of LIF and its cognate cell surface receptor subunits, LIFR and gp130, become transiently elevated following injury and are enriched in nonparenchymal cell fractions containing stem/progenitors.[37]

Intracellular staining patterns to define rHpSCs and rHBs were assessed by comparative analysis of qRT-PCR data derived from similarly treated cultures. In response to LIF, cultures had comparatively higher mRNA expression of *Afp* and *Alb* and other markers indicating marked rHB growth. Expression levels of markers specific to rHpSCs (*Ncam*), of those found in both rHpSCs and rHBs (*Sox9*), or in both but enriched in rHpSCs (*Epcam*) were similar between LIF– and LIF+ cultures. Thus, gating of colonies based on E-cadherin and ALB expression provided

accurate distinctions between rHpSCs and rHBs and were used to examine treatment-related effects on distinct stages of stem/progenitors.

The novel culture system enabled evaluation of AHR agonist effects on rHpSCs versus rHBs. AHR is activated by structurally diverse ligands (Fig. S1). TCDD is an environmental pollutant which is poorly metabolized by mammalian liver cells and is one of the most potent AHR agonists known.[4] FICZ is a tryptophan photodegradation byproduct rapidly metabolized in mammalian liver cells and with a similar potency for AHR activation as that of TCDD.[4] DIM is an indole-3-carbanol derivative in cruciferous vegetables and is a much less potent AHR agonist compared to either TCDD or FICZ.[4] Using *Cyp1a1* expression as a measure of AHR activation,[1] differences in potency and efficacy were observed among the three ligands. A persistent increase in *Cyp1a1* expression (~500-fold) was observed between 24-96 hours postexposure at all TCDD concentrations examined (0.1-100 nM). In contrast, FICZ produced a transient increase in *Cyp1a1* expression at 0.1 and 1 nM and a persistent increase at 10 and 100 nM (~70 to 120-fold). DIM produced a persistent increase in *Cyp1a1* expression at 1 and 10 μM, although the efficacy (~9-50-fold) was lower than that observed with either TCDD or FICZ. The differences in potency between the three ligands were consistent with previous reports.[4]

The persistent increase in *Cyp1a1* expression by TCDD and DIM indicated that these compounds may be poorly metabolized by rat hepatic stem/progenitors. By comparison, the transient increase in *Cyp1a1* expression observed with lower concentrations of FICZ (0.1 and 1 nM) indicated that this ligand may be metabolized by rat hepatic stem/progenitors at a rate similar to that observed in mature liver cells.[38] It is possible that at higher FICZ concentrations (10-100 nM), the metabolic capacity of the cells is saturated for the treatment paradigm employed (i.e., dose every 3 days), leading to AHR activation for the duration of the experiment.

All three AHR ligands stimulated rHpSC colony growth. However, effects on rHBs were strong by TCDD and more muted by FICZ and DIM. An inverted concentration-response was observed for TCDD in terms of promoting rHpSC colony growth, with 0.1 and 1 nM TCDD being most effective. The number of rHB colonies as well as the mean rHB colony area was decreased at all TCDD concentrations. DIM at 1 and 10 μM had similar effects on rHpSC and rHB colony growth as compared to TCDD. FICZ demonstrated distinct characteristics in which FICZ (1-100 nM) stimulated rHpSC colony growth but had no effect on rHB colony growth at any concentration tested. The underlying cause(s) is unknown but may be due to differences in potency, efficacy for AHR activation, or differences in metabolism across compounds. Alternatively, depletion or down-regulation of AHR has also been observed following acute, *in vivo* exposure to TCDD.[39] The effects of TCDD and DIM at higher concentrations on rHB growth could potentially be due to AHR depletion. Overall, high-content imaging and gene expression data supported that activation of AHR has a stimulatory effect on growth of rHpSCs and loss of viability of rHBs.

Expression patterns of hepatic stem/progenitor markers were consistent with rHpSC versus rHB growth patterns observed using high-content imaging. Patterns of mRNAs in conditions stimulating rHpSC growth (increases in *Epcam* and *Sox17*; decreases in *Alb* or *Afp*) correlated with increases in rHpSC growth measured in imaging experiments. A similar relationship between high-content imaging and gene expression data was observed for inhibition of rHB growth. Decreases in *Afp* and *Alb* mRNA expression were observed in instances where marked rHB growth inhibition occurred, as with TCDD. Modest decreases in rHBs growth, as with higher concentrations of DIM, did not produce a concomitant decrease in either *Alb* or *Afp*, confirming that the expression of these genes correlated with inhibition or absence of rHB growth. Although FICZ caused increases in *Epcam* and, at the highest concentration, elevated *Sox17* and lowered *Alb*, it also resulted in modestly elevated *Afp*, a finding perhaps related to FICZ metabolism in the cells.

Sox17, an endodermal transcription factor, found consistently in hHpSCs, was variably expressed in rHpSCs and not at all in hHBs or rHBs. SOX17's highest levels have been found in BTSCs.[40] In rats, perhaps expression of SOX17 is restricted to BTSCs and is not a robust marker for rHpSCs, an hypothesis being tested. Increased *Sox17* mRNA expression was observed in three of seven conditions in which a significant stimulation of rHpSC growth was observed and in two conditions in which rHpSC colony losses occurred (i.e., 10 and 100 nM TCDD). The reason for the discordance is unclear.

Lineage-stage-specific effects of TCDD on rHpSC and rHB colonies provide insight into a mode-of-action for TCDD-induced liver tumorigenesis. In 2-year cancer bioassays, female rats were chronically exposed to TCDD, causing increased incidences of

hepatocytic and cholangiocytic tumors and increased stem/progenitor cell proliferation (i.e., an oval cell response).[8,9] Given the ability of rHpSCs and rHBs to differentiate towards either an hepatocytic or cholangiocytic fate, the effects of TCDD implicate a malignant transformation of either one or both. Studies with WB-F344 cells suggested that TCDD can release cells from contact-inhibition-mediated cell cycle arrest and alter expression of cell cycle genes and adhesion molecules.[10,19-21,41] These results have been interpreted as consistent with activity of TCDD as a nongenotoxic liver tumor promoter. Our studies implicate a more complex, lineage-dependent mechanism in which TCDD stimulates growth of rHpSCs and, in parallel, causes loss of viability of rHBs. This results in a loss of feedback loop signals that influences the rHpSCs to remain quiescent.[16,42] Increased proliferation of rHpSCs could result in an increased likelihood of acquiring deleterious mutations that could contribute to oncogenesis. The toxic and carcinogenic potential of the other two AHR ligands examined, FICZ and DIM, are considered less than that of TCDD due to differences in potency, metabolism, and clearance.[4] Our findings implicate the importance of lineage-dependent mechanisms of chemical toxicities and their influence on liver biology and pathobiology.

Acknowledgment: The Hamner Studies were funded by the Dow Chemical Company (Midland, MI). UNC: L.M.R.'s funding derived from a subcontract from the Hamner's grant from the Dow Chemical Company, from Vesta Therapeutics (Bethesda, MD), and from an NIH grant (R21CA182322). Core support services were provided by an NIH Cancer Center grant (CA016086). Glassware washing assistance was provided by Lucendia English.

References

1. Denison MS, Soshilov AA, He G, DeGroot DE, Zhao B. Exactly the same but different: promiscuity and diversity in the molecular mechanisms of action of the aryl hydrocarbon (dioxin) receptor. Toxicol Sci 2011;124:1-22.
2. Kolluri SK, Weiss C, Koff A, Gottlicher M. Induction and inhibition of prolieration by the intracellular Ah receptor in developing thymus and heptoma cells. Genes Dev 1999;13:1742-1753.
3. Ma Q, Baldwin KT, Renzelli AJ, McDaniel A, Dong L. TCDD-inducible poly (ADP-ribose) polymerase: a novel response to 2,3,7,8-tetrachlorodibenzo-p-dioxin. Biochem Biophys Res Commun 2001;289: 499-506.
4. Nguyen LP, Bradfield CA. The search for endogenous activators of the aryl hydrocarbon receptor. Chem Res Toxicol 2008;21:102-116.
5. Schroeder JC, Dinatale BC, Murray IA, Flaveny CA, Liu Q, Laurenzana EM, et al. The uremic toxin 3-indoxyl sulfate is a potent endogenous agonist of the human aryl hydrocarbon receptor. Biochemistry 2010;49:393-400.
6. Fernandez-Salguero PM, Hilbert DM, Rudikoff S, Ward JM, Gonzalez FJ. Aryl-hydrocarbon receptor-deficient mice are resistant to 2,3,7.8-tetrachlorodibenzo-p-dioxin-induced toxicity. Toxicol Appl Pharmacol 1996;140:173-179.
7. Peters JM, Narotsky MG, Elizondo G, Fernandez-Salguero PM, Gonzalez FJ, Abbott BD. Amelioration of TCDD-induced teratogenesis in aryl hydrocarbon receptor (AhR)-null mice. Toxicol Sci 1999;47.
8. NTP Technical Report on the Toxicology and Carcinogenesis Studies of 2,3,7,8,-Tetrachlorodibenzo-p-dioxin (TCDD) in Female Harlan Sprague-Dawley Rats. National Toxicology Program Technical Report Series 2006;5:4-232.
9. Kociba RJ, Keyes DG, Beyer JE, Carreon RM, Wade CE, Dittenber DA, et al. Results of a two-year chornic toxicity and oncogenicityi study of 2,3,7,8-tetrachlorodibenzo-p-dioxin in rats. Toxicol Appl Pharmacol 1978;46:279-303.
10. Feng S, Cao Z, Wang X. Role of aryl hydrocarbon receptor in cancer. Biochim Biophys Acta 2013;1836:197-210.
11. Budinsky RA, Schrenk D, Simon T, Van den Berg M, Reichard JF, Silkworth JB, et al. Mode of action and dose-response framework analysis for receptor-mediated toxicity: the aryl hydrocarbon receptor as a case study. Crit Rev Toxicol 2014;44:83-119.
12. **Cardinale V**, **Wang Y**, Carpino G, Cui CB, Gatto M, Rossi M, et al. Multipotent stem cells in the extrahepatic biliary tree give rise to hepatocytes, bile ducts and pancreatic islets. HEPATOLOGY 2011;54:2159-2172.
13. **Schmelzer E**, **Zhang L**, Bruce A, Wauthier E, Ludlow J, Yao HL, et al. Human hepatic stem cells from fetal and postnatal donors. J Exp Med 2007;204:1973-1987.
14. Turner R, Lozoya O, Wang YF, Cardinale V, Gaudio E, Alpini G, et al. Hepatic stem cells and maturational liver lineage biology. HEPATOLOGY 2011;53:1035-1045.
15. Wang Y, Yao H, Cui C, Wauthier E, Barbier C, Costello M, et al. Paracrine signals from mesenchymal cell populations govern the expansion and differentiation of human hepatic stem cells to adult liver fates. HEPATOLOGY 2010;52:1443-1454.
16. Furth ME, Wang Y, Cardinale V, Carpino G, Lanzoni G, Cui C, et al. Stem cell populations giving rise to liver, biliary tree and pancreas. In: Sell S, editor. The stem cells handbook, 2nd ed. New York: Springer Science Publishers; 2013. p 75-126.
17. Cardinale V, Wang Y, Gaudio E, Mendel G, Alpini G, Gaudio E, et al. The biliary tree: a reservoir of multipotent stem cells. Nat Rev Gastroenterol Hepatol 2012;9:231-240.
18. Tsao MS, Smith JD, Nelson KG, Grisham JW. A diploid epiothelial cell line from normal adult rat liver with phenotypic properties of 'oval' cells. Exp Cell Res 1984;154:38-52.
19. Dietrich C, Faust D, Budt S, Moskwa A, Kunz A, Bock K, et al. 2,3,7,8-Tetrachlorodibenzo-p-dioxin-dendent release from contact inhibition in WB-F344 cells: involvement of cyclin A. Toxicol Appl Pharmacol 2002;183:117-126.
20. Prochazkova J, Kabatkova M, Bryja V, Umannová L, Bernatík O, Kozubík A, et al. The interplay of the aryl hydrocarbon receptor and bveta-catenin alters both AhR-dependent transcription and Wnt/beta-catenin signaling in liver progenitors. Toxicol Sci 2011;122:249-360.
21. Umannova L, Zatloukalova J, Machala M, Krcmár P, Májková Z, Hennig B, et al. Tumor necrosis factor-alpha modulates effects of arylo hydrocarbon receptor ligands on cell proliferation and expression of cytochrome P450 enzymes in rat liver "stem-like" cells. Toxicol Sci 2007;99:79-89.
22. Kubota H, Reid LM. Clonogenic hepatoblasts, common precursors for hepatocytic and biliary lineages, are lacking classical major histocompatibility complex class I antigens. Proc Natl Acad Sci U S A 2000;97: 12132-12137.
23. Livak KJ, Schmittgen TD. Analysis of relative gene expression data using real-time quantitative PCR and the 2 (-Delta Delta C (T)) method. Methods 2001;25:402-408.
24. Barbaric I, Gokhale PJ, Jones M, Glen A, Baker D, Andrews PW. Novel regulators of stem cell fates identified by a multivariate phenotype screen of small compounds on human embryonic stem cell colonies. Stem Cell Res 2010;5:104-119.

25. Kubota H, Yao H, Reid LM. Identification and characterization of vitamin A-storing cells in fetal liver. Stem Cell 2007;25:2339-2349.
26. Darzynkiewicz Z, Balaszs EA. Genome integrity, stem cells and hyaluronan. Aging 2012;4:78-88.
27. Goodison S, Urquidi V, Tarin D. CD44 cell adhesion molecules. Mol Pathol 1999;52:189-196.
28. Schmidt DS, Klingbell P, Schnolzer M, Zoller M. CD44 variant isoforms associate with tetraspanins and EpCAM. Exp Cell Res 2004;297: 329-347.
29. Hirohashi K, Yamamoto T, Uenishi T, Ogawa M, Sakabe K, Takemura S, et al. CD44 and VEGF expression in extrahepatic metastasis of human hepatocellular carcinoma. Hepatogastroenterology 2004;51: 1121-1123.
30. Kuhn S, Koch M, Nubel T, Ladwein M, Antolovic D, Klingbeil P, et al. A complex of EpCAM, claudin-7, CD44 variant isoforms, and tetraspanins promotes colorectal cancer progression. Mol Cancer Res 2007;5:553-567.
31. Yang GH, Fan J, Xu Y, Qiu SJ, Yang XR, Shi GM, et al. Osteopontin combined with CD44, a novel prognostic biomarker for patients with hepatocellular carcinoma undergoing curative resection. Oncologist 2008;13:1155-1165.
32. Ogawa M, Yamamoto T, Kubo S, Uenishi T, Tanaka H, Shuto T, et al. Clinicopathologic analysis of risk factors for distant metastasis of hepatocellular carcinoma. Hepatol Res 2004;29:228-234.
33. Wang M, Xiao J, Shen M, Yahong Y, Tian R, Zhu F, et al. Isolation and characterization of tumorigenic extrahepatic cholangiocarcinoma cells with stem cell-like properties. Int J Cancer 2011;128:72-81.
34. Chiu CC, Sheu JC, Chen CH, Lee CZ, Chiou LL, Chou SH, et al. Global gene expression profiling reveals a key role of CD44 in hepatic oval-cell reaction after 2-AAF/CCl4 injury in rodents. Histochem Cell Biol 2009;132:479-489.
35. Hirai H, Firpo M, Kikyo N. Establishment of LIF-dependent human iPS cells closely related to basic FGF-dependent authetic iPS cells. PLoS One 2012;7:e39022.
36. Hilton DJ, Nicola NA, Waring PM, Metcalf D. Clearance and fate of leukemia-inhibitory factor (LIF) after injection into mice. J Cell Physiol 1991;148:430-349.
37. Omori N, Evarts RP, Omori M, Hu Z, Marsden ER, Thorgeirsson SS. Expression of leukemia inhibitory factor and its receptor during liver regeneration in the adult rat. Lab Invest 1996;75:15-24.
38. Bergander L, Wincent E, Rannug A, Foroozesh M, Alworth W, Rannug U. Metabolic fate of the Ah receptor ligand 6-formylindolo[3,2-b] carbazole. Chem Biol Interact 2004;149:151-164.
39. Pollenz RS, Santostefano MJ, Klett E, Richardson VM, Necela B, Birnbaum LS. Female Sprague-Dawley rats exposed to a single oral dose of 2,3,7,8-tetrachlorodibenzo-p-dioxin exhibit sustained depeletion of aryl hydrocarbon receptor protein in liver, spleen, thymus and lung. Toxicol Sci 1998;42:117-128.
40. Wang Y, **Lanzoni G**, **Carpino G**, Cui CB, Dominguez-Bendala J, Wauthier E, et al. Biliary tree stem cells, precursors to pancreatic committed progenitors: evidence for life-long pancreatic organogenesis. Stem Cells 2013;31:1966-1979.
41. Weiss C, Faust D, Schreck I, Ruff A, Farwerck T, Melenberg A, et al. TCDD deregulates contact inhibition in rat liver oval cells via Ah receptor, JunD and cyclin A. Oncogene 2008;27:2198-2207.
42. Yimlamai D, Christodoulou C, Galli GG, Yanger K, Pepe-Mooney B, Gurung B, et al. Hippo pathway activity influences liver cell fate. Cell 2014;157:1324-1338.

Author names in bold designate shared co-first authorship.

Supporting Information

Additional Supporting Information may be found at onlinelibrary.wiley.com/doi/10.1002/hep.27547/suppinfo.